Hydraulic and thermal behaviors of diabatic two-phase flow through porous particle beds

Dong Ju Lee [a], Jong Seok Oh [a], Sang Mo An [b], Hwan Yeol Kim [b], Dong Eok Kim [a*]
[a]*School of Energy System Engineering, Chung-Ang University, Seoul 06974, Korea*
[b]*Korea Atomic Energy Research Institute, 111, Deadeok-daero 989 beon-gil, Yuseong-gu, Daejeon 34057, Korea*
**Corresponding author: dekim@cau.ac.kr*

1. Introduction

The behaviors of two-phase flow through porous particle beds have been studied for decades in various industrial and engineering fields. Particularly in a nuclear reactor under the severe accident condition, the two-phase flow phenomena through the particle bed can be a critical issue for reactor safety. Therefore, a basic understanding of the relevant hydrodynamics with two-phase flow accompanying phase-change process through the porous particle beds is essential to the reactor safety analysis. In this study, we conducted the experiments for saturated steam-water flow (boiling) in various particle beds. The experimental data of two-phase pressure drop and dryout heat flux (DHF) were analyzed with the numerical results from existing hydrodynamic models and previous correlations.

2. Methods

2.1 Experimental

Fig. 1 illustrates the experimental design. The particle beds formed within the cylindrical test section made of STS304 pipe (ID: 110 mm, thick.: 15 mm, and L: 400 mm). The test section was installed inside a rectangular water pool (inner dimension: $360 \times 360 \times 660$ mm^3). Four visualization windows made of transparent polycarbonate (PC windows) were mounted to the sides of the water pool. For heating the particle beds, twelve cartridge heaters (OD: 9.42 mm, L: 450 mm, Power: 2.0 kW) were inserted from the bottom of the test section at the same spacing of 25 mm (see Fig. 1). The thermal power (P_t) to the particle beds was controlled using two AC power controllers, and was measured using the AC voltage and current meters, i.e., $P_t = V_s I_s$ where V_s and I_s are the voltage and current values applied into the heaters. The heat flux (q_b) with respect to the cross-sectional area of the particle bed is calculated as $q_b = P_t/A_s$ where A_s is the cross-sectional area excluding the internal structures in the test section, such as the cartridge heaters and thermocouples. Note that the experimental setup has an inherent limitation to simulate the real phenomena where the individual porous particles generate heat. For local temperature measurements and DHF (q_d) detection, a total of thirty K-type thermocouples were inserted into the test section in both the axial and radial directions (see Fig. 1). q_d is defined as the heat flux at which the local overheating within the particle beds occurs. The boiling experiments were conducted under a saturated condition (saturation temperature: $T_{sat} = 100$ ℃) at the atmospheric pressure, and tap water was used as the working fluid. The two-phase pressure through the particle bed and the absolute pressure at the bottom of the bed were measured using the pressure tabs at the top and bottom of the test section and the absolute and differential pressure transmitters. Table I and II list the operating and design conditions of the experiments, and test cases and specifications of the particle beds, respectively.

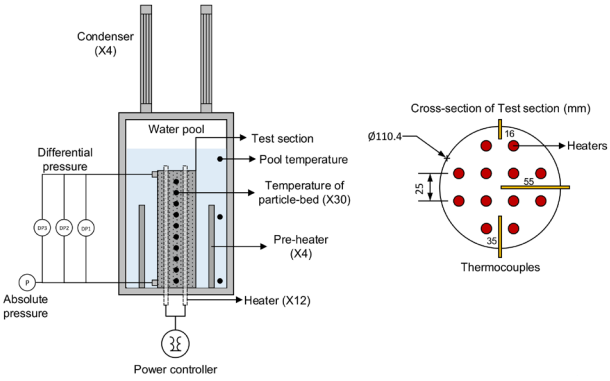

Fig. 1. Schematic of diagram of the experimental facility.

Table I: Operating and design conditions of saturated boiling experiments.

Fluid condition	Electric power (kW)	Vapor superficial velocity (m/s)	Heat flux (MW/m^2)
Saturated at 1 atm	Operating: 0-17 Design: 0-24	Operating: 0-1.5 Design: 0-2.15	Operating: 0-2.0 Design: 0-2.87

Table II: Experimental cases and specifications of the particle beds.

Case	Particle diameter, D_p (mm)	Porosity (ε)
BO-DP1	1	0.409
BO-DP3	3	0.409
BO-DP5	5	0.427
BO-DP6	6	0.428
BO-TROI	TROI distribution [1]	0.355

2.2 Models and numerical methods for analyzing the experimental data

To analyze the model predictions for the two-phase pressure loss and DHF behaviors under the boiling condition, we solved numerically the steady-state one-dimensional momentum equations shown in Eqs. (1)-(3).

$$-\frac{dP_g}{dz} = \rho_g g + \frac{\mu_g}{KK_{rg}} J_g + \frac{\rho_g}{\eta\eta_{rg}} J_g \left|J_g\right| + \frac{F_i}{\alpha}, \quad (1)$$

$$-\frac{dP_l}{dz} = \rho_l g + \frac{\mu_l}{KK_{rl}} J_l + \frac{\rho_l}{\eta\eta_{rl}} J_l \left|J_l\right| - \frac{F_i}{1-\alpha}, \quad (2)$$

$$\frac{dP_g}{dz} = \frac{dP_l}{dz}, \tag{3}$$

where P, z, ρ, g, μ, K, η, J, K_r, η_r, F_i, α, subscripts g and l are the fluid pressure, one-dimensional coordinate in upward direction, fluid density, gravity acceleration, dynamic viscosity, permeability, passability, fluid superficial velocity, relative permeability, relative passability, interfacial drag force (unit: N/m^3), void fraction, vapor and liquid, respectively. In addition to Eqs. (1)-(3), the continuity equation based on the mass and energy balance due to the phase-change was used, i.e., $\rho_g J_g + \rho_l J_l = 0$. In the previous studies [2-10], different types of the relations for K_r, η_r, and F_i were applied into Eqs. (1) and (2) depending on the relevant flow regime. In this study, we adopted three types of the models for the two-phase pressure loss through the porous particle beds, i.e., Schulenberg and Müller model [3] (SM model), Tung and Dhir model [4] (TD model), and Schmidt model [2] (SC model). We developed the in-house codes written in MATLAB R2020a for solving the pressure balance equation from Eq. (3) based on the SM, TD, and SC models. Additionally, we compared the DHF data in the experimental cases with the previous correlations for counter-current flooding limit (CCFL) proposed by Wallis [11] and Schrock et al. [12].

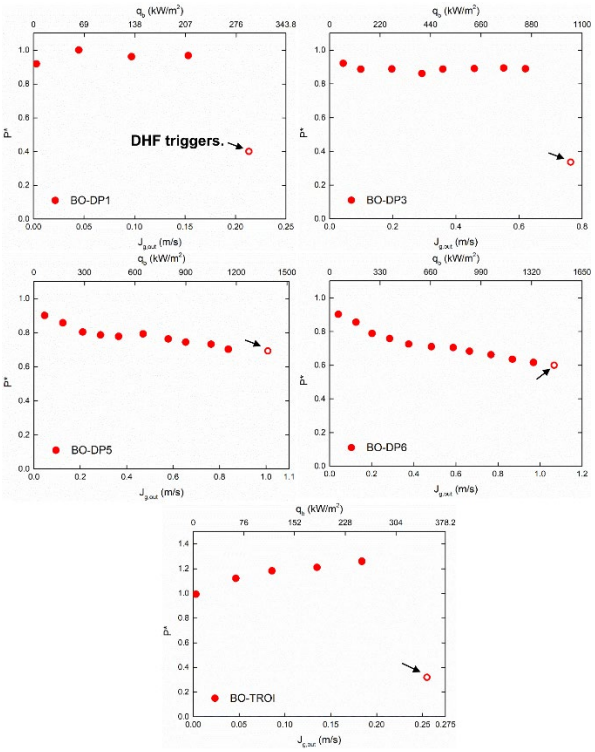

Fig. 2. Non-dimensional pressure gradients and DHFs in the boiling experiments ($J_{g,out}$: J_g at the outlet).

3. Results and discussion

As shown in the Table II, we conducted the saturated boiling experiments for the four types of uniform particle beds and non-uniform particle bed with the TROI distribution [1]. Fig. 2 shows the behaviors of non-dimensional pressure gradient (P^*, Eq. (4)) in the boiling experiments.

$$P^* = \frac{-dP/dz}{(\rho_l - \rho_g)g}. \tag{4}$$

The hollow circles in the plots presented in Fig. 2 indicate the conditions at which the DHF (q_d) phenomenon was triggered. The values of q_d increases with D_p. In the cases of BO-DP1 and BO-DP3, the sudden drop of P^* was observed, and it indicates the local flow regime transition from two-phase to single-phase vapor flow within the pores. For the cases of larger particles (BO-DP5 and BO-DP6), the transition might be milder than the former cases. Fig. 3 shows the transient variations of the local fluid temperatures (using 30 thermocouples) in the particle beds at q_d. In the particle bed under normal boiling condition, the local fluid temperatures were maintained near the saturation temperature (100 °C). However, they exhibit a significant temporal increase under the dryout heat flux conditions. In BO-DP5 case, a maximum rate of local temperature increase was recorded to 0.9 °C/s. As shown in the temperature contours (see the insets of Fig. 3), the dryout triggers at the local position in the particle beds, and it expands temporally. Interestingly, the local dryout was detected simultaneously at several local positions in the BO-TROI case. The DHF triggering position rises up as the particle diameter increases for the uniform particle beds.

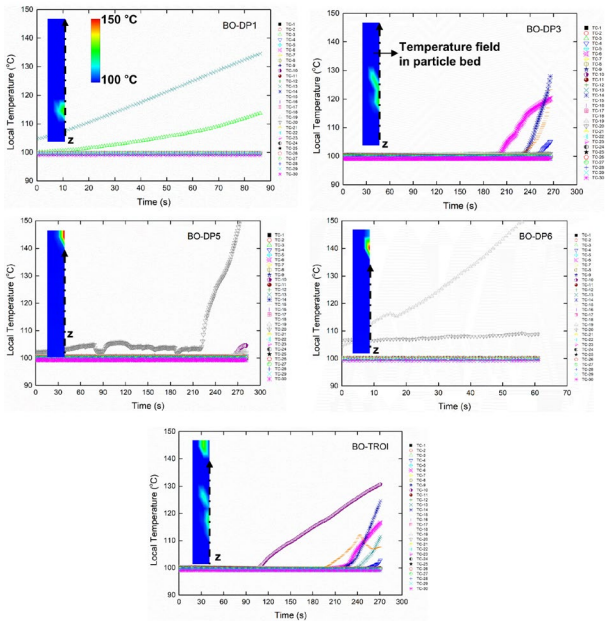

Fig. 3. Temporal variations of local fluid temperatures in the particle beds under DHF conditions.

We analyzed the model predictions for the two-phase pressure loss and DHF behaviors using the numerical codes based on SM, TD, and SC models. For considering

the spatial variations of J_g, α and flow regime through the particle beds under the phase-change condition, the calculation domain (particle beds) was divided into the 40 grid points (grid spacing: 10 mm) as shown in Fig. 4. In this figure, the experimental P^* data were compared with the predictions from SM, TD, and SC models. The predicted P^* data obtained by spatially averaging the P^* values at the grid points. For the uniform particle beds with relatively small D_p (BO-DP1 and BO-DP3 cases), the SC model shows very good agreements with the experimental P^* and q_d data. q_d values predicted by the models are marked with the × symbols in the plots. For the larger D_p cases (BO-DP5 and BO-DP6), the models slightly underestimate the P^* from the experiments, and show qualitative agreements with the variation trends of experimental P^*. Overally, the TD model underestimates the experimental q_d. In the plot for the BO-TROI case, an unusual trend of the experimental P^* is shown. Theoretically, the one-dimensional steady-state and stable two-phase flow within the particle beds cannot be maintained under the condition $P^* > 1$. For the results, we guess that the multi-dimensional flow path may have formed within the particle bed due to the random packing of the particles with broadly distributed D_p.

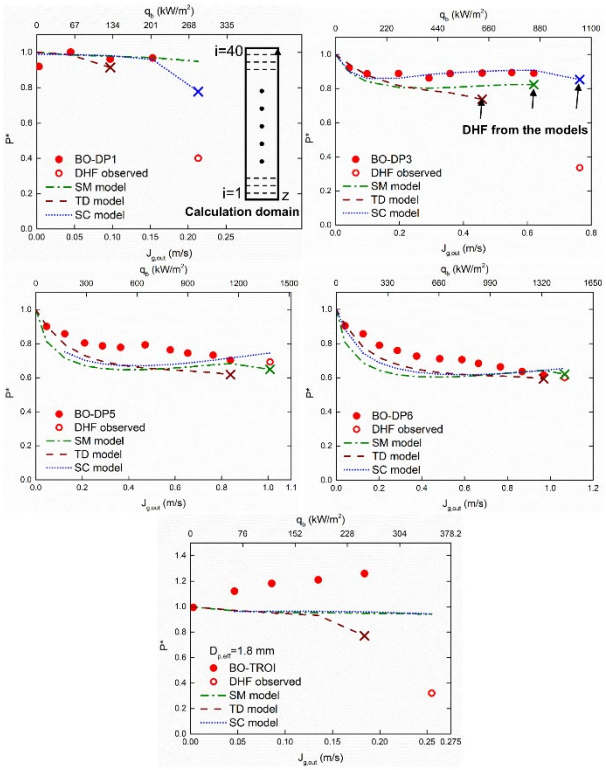

Fig. 4. Experimental and model prediction results for the non-dimensional pressure gradients and DHFs in the boiling experiments.

Fig. 5 shows the DHF prediction results of existing models with the present experimental data. For the SM, TD, and SC models, the DHF was defined as the heat flux at which the CCFL occurs at the top of the particle bed.

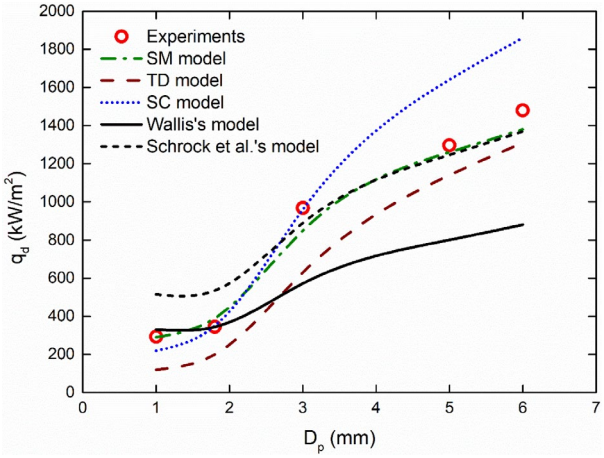

Fig. 5. Comparison of experimental DHFs and predictions from the previous models.

The SM model shows the best estimations to the experimental q_d data with the variation of D_p, while the SC model shows good agreements with the experiments for the cases of D_p smaller than 3 mm and overestimates the values of q_d for the large D_p (=5 and 6 mm) cases. The TD model underestimates overally the experimental data. The DHF values for the fine particle beds ($D_p <$ 3 mm) agreed well with the Wallis model [11] in which only gas and liquid drag forces were considered into the model relation. The classical simplified models for the CCFL prediction from Wallis [11] (for the cases of $D_p \geq$ 3 mm) and Schrock et al. [12] show the large deviations from the experimental data in both qualitative and quantitative manners. In the classical models, the CCFL phenomenon was simplified with the relationship between the gas and liquid inertial drag forces and the gravity force, i.e., the viscous and interfacial drag forces were not considered properly in the model.

4. Conclusions

The results of this study can be summarized as below:

- In the saturated boiling experiments through various particle beds, the two-phase pressure gradient through the beds continuously decreased with J_g before the occurrence of DHF phenomenon.
- With the onset of DHF, rapid increments of the local fluid temperatures in the particle beds were observed (maximum rate of local temperature increase: 0.9 °C/s). The existing models showed reasonably good agreements with the experimental pressure loss data, and the SM model predicted the DHF results best.

REFERENCES

[1] H.Y. Kim, K.H. Park, K.S. Choi, C.W. Kang, J.H. Jung, S.M. An, Analysis of non-explosive TROI particles for debris-bed coolability study, Trans. KNS Virt. Autum. Mtg., Dec., 2019.

[2] W. Schmidt, Influence of multidimensionality and interfacial friction on the coolability of fragmented corium, Ph. D. Thesis, Univ. Stuttgart, 2004.

[3] T. Schulenberg, U. Müller, An improved model for two-phase flow through beds of coarse particles, Int. J. Multiphas. Flow Vol. 13, pp. 87-97, 1987.
[4] V.X. Tung, V.K. Dhir, A hydrodynamic model for two-phase flow through porous media, Int. J. Multiphas. Flow Vol. 14, pp. 47-65, 1988.
[5] K. Hu, T.G. Theofanous, On the measurement and mechanism of dryout in volumetrically heated coarse particle beds, Int. J. Multiphas. Flow, Vol. 17, pp. 519-532, 1991.
[6] R.J. Lipinski, A model for boiling and dryout in particle beds, No. NUREG/CR-2646, Sandia National Labs., 1982.
[7] N.K. Tutu, T. Ginsberg, J.C. Chen, Interfacial drag for two-phase flow through high permeability porous beds, J. Heat Transfer, Vol. 106, pp. 865-870, 1984.
[8] A.S. Naik, V.K. Dhir, Forced flow evaporative cooling of a volumetrically heated porous layer, Int. J. Heat Mass Tran., Vol. 25, pp. 541-552, 1982.
[9] J.H. Park, H.S. Park, M. Lee, K. Moriyama, Modeling of pressure drop in two-phase flow of mono-sized spherical particle beds, Int. J. Heat Mass Tran., Vol. 127, pp. 986-995, 2018.
[10] D.Y. Yeo, H.C. No, A zero-dimensional dryout heat flux model based on mechanistic interfacial friction models for two-phase flow regimes with channel flow in a packed bed, Int. J. Heat Mass Tran. Vol. 141, pp. 554-568, 2019.
[11] G.B. Wallis, One-dimensional two-phase flow, McGraw-Hill, New York, 1969.
[12] V.E. Schrock, C.H. Wang, S. Revankar, L.H. Wei, S.Y. Lee, D. Squarer, Flooding in particle beds and its role in dryout heat fluxes, Proc. 6th Inform. Exchan. Mtg. on Debris Coolability, UCLA, Los Angeles, 1984.